IMPACT OF LEAD RUBBER BEARING BASE ISOLATION SYSTEMS ON BUILDING STRUCTURES DESIGNED AS PER EUROCODE 8

Mohammed Tamahloult[1], Mouloud Ouanani[2], Boualem Tiliouine[1]*

[1]Laboratory of Earthquake Engineering and Structural Dynamics, Department of Civil Engineering, Ecole Nationale Polytechnique, Algeria
[2]Department of Civil Engineering, University of Djelfa, Algeria

*Corresponding author's e-mail: boualem.tiliouine@g.enp.edu.dz

Abstract

Introduction: Seismic base isolation has been classified as a structural protection system designed to minimize the seismic forces transferred to a structure during an earthquake. This can be achieved through the use of various devices, such as elastomeric bearings, sliding bearings, and hybrid systems. **Purpose of the study**: The study aims to evaluate the impact of using lead rubber bearings (LRB) as a base isolation system in building structures. **Methods:** In order to achieve this, nonlinear dynamic analyses of a seven-story building with and without an isolation device at its base were performed using the Fast Nonlinear Analysis (FNA) algorithm. The building was designed according to Eurocode 8 (EC8) criteria and then subjected to analysis using data from two previous earthquake events. **Results**: It is concluded that the bilinear behavior assumption made in the design stage according to EC8 is appropriate. Additionally, implementing an isolation system with LRBs at the building foundation can significantly enhance building performance by reducing floor accelerations, inter-story drifts, and base shear responses. Furthermore, it is demonstrated that isolating a building at its base with LRBs effectively reduces internal forces due to both gravity and seismic loads.

Keywords: base isolation; LRB system; 3D nonlinear earthquake response analysis; Eurocode 8; bilinear hysteresis.

Introduction

Seismic isolation is an excellent method for passive protection of a building structure. It enhances structural performance and reduces potential earthquake damage by lengthening the fundamental period of vibration and increasing energy dissipation (Naeim and Kelly, 1999). Seismic base isolation systems, including laminated rubber bearings, friction pendulum systems, and Teflon-steel friction bearings, have been utilized to reduce the transmission of seismic forces from the ground to a building structure.

Each of these systems has its own characteristics and advantages. Laminated rubber bearings are known for their durability, cost-effectiveness, and optimal control of their characteristics (Jain et al., 2004).

A laminated rubber bearing consists of alternating thin layers of rubber and steel, giving it the ability to support heavy weights due to its stiffness in the vertical direction. At the same time, it is horizontally flexible, allowing superstructures to move similarly to the motion of a rigid body during an earthquake (Koo et al., 1999). A lead rubber bearing (LRB) is a specific type of the laminated rubber bearing that includes a lead core in its structure, providing high initial rigidity and high damping, with equivalent damping varying from 15 to 35 % (Attanasi et al., 2009). Buildings equipped with LRBs demonstrated excellent performance during past earthquakes

(1994 — Northridge; 1995 — Kobe), confirming the effectiveness of LRBs as suitable base isolators (Asher et al., 1997).

Several mathematical models have been used to characterize the hysteresis behavior of various types of bearings. The idealized hysteresis behavior of bearings has been the subject of extensive studies. Among the various models proposed, the bilinear model is widely used in both research and design practice (e.g. Amanollah et al., 2023). Its simplicity allows for an accurate characterization of the mechanical properties of bearings, making it suitable for both elastomeric-type and sliding-type bearings (Cheng et al., 2008).

According to Mayes (Mayes and Naeim, 2001), any design process must ensure that (i) the bearings will safely withstand the maximum gravity service loads for the lifetime of the structure and (ii) provide period shift and hysteretic damping during one or more design earthquakes.

The current generation of building codes has progressed in two significant ways. Firstly, they provide guidelines for incorporating energy dissipation mechanisms, taking into consideration both the lateral strength method and the type of structural material used. Secondly, these updated codes have expanded their scope to include additional considerations, such as geotechnical aspects. Furthermore, these new regulations incorporate a semi-probabilistic approach to assess safety, in line with the principles defined

in EN 1990 (Elghazouli, 2009). Eurocode 8 (European Committee for Standardization, 2004) includes a dedicated chapter on the seismic isolation of buildings and bridges. In that chapter, the calculation of maximum isolator displacement is carried out in the preliminary design phase using the Equivalent Linear Force (ELF) method (Cavdar and Ozdemir, 2022). In the same context of designing building structures with base isolation, the Chinese code GB50011-2010 (Ministry of Housing and Urban-Rural Development of the People's Republic of China, 2010) recommends a distinct design approach. This approach ensures that the isolation system and superstructure are designed independently, and introduces the concept of horizontal seismic isolation coefficients (Hu et al., 2023).

In this study, we aim to demonstrate the impact of seismic base isolators on building structures during earthquakes. The analyses were carried out on a multi-story building model with a base isolation system with LRBs incorporated at the base, as well as on the same model with a fixed base, both designed according to EC8. The earthquake data included ground motion records from the 1940 El Centro and the 1996 Kobe earthquakes.

Subject, models, and methods

Building model

The subject model is a seven-story frame building with dimensions of 15×8 m². The beam sections are 40×30 cm², and the column sections are 50×50 cm². Each story has a height of 3 m, as shown in Fig. 1a and Fig. 1b. The building is isolated with LRBs placed under each column between the foundation and superstructure, and attached to a 10 cm rigid base slab. The total weight of the building is 14.066 kN. The fundamental period of the building is 0.61 s, and the modal damping ratio is expected to remain constant at 5 % for each mode. The building structure is intended to be located in a highly seismic zone, resting on a soil profile categorized as stiff soil profile

type C. The system isolator to be used is a lead rubber bearing (LRB) as shown in Fig. 2. Two LRB profiles are designed for the building because the gravity load transferred to the corner bearings is less than that transferred to the inner and side bearings.

The bearings are labeled as *(A)* for the columns at the corners and *(B)* for those on the sides and inside (Fig. 1b). The force deformation behavior of the isolators (LRBs) in this study is modeled as a nonlinear hysteretic loop directly idealized by the bilinear model (AASHTO, 2010; Kelly, 1997; Mori et al., 1998) as indicated in Fig. 3.

Seismic displacement criteria as per EC8

First, we define the design response spectrum of each isolator (LRB^A, LRB^B) in accordance with the seismic requirements specified by Eurocode 8, Type 1 spectrum (Fig. 4). This applies to areas with high seismicity and near-field earthquakes, relative to a reference peak ground acceleration (PGA) of a_{gR} = 0.4 g. The importance factor for the building g_I = 1; soil type — C, spectral parameters from EC8 (Table 3.2) are as follows:

$T(s)$ is the linear *SDOF* system's vibration period and *Se(T)* is the elastic response spectrum; the lower and upper limits of the period of the constant spectral acceleration branch are T_B = 0.2 s and T_C = 0.6 s, respectively. Soil factor S = 1.15. Damping correction factor η = 0.7.

The desired effective period (T_{eff}) and effective damping (ξ_{eff}) of the isolation system are assumed to be T_{eff} = 2 s and ξ_{eff} = 0.137, respectively. Following a gravity load analysis, we determine that the vertical reaction is as follows: R^a = 989 kN for the corner columns and R^b = 1.461 kN for the side and inside columns. Subsequently, the effective stiffness of each rubber isolation bearing is defined as follows:

$$K_{eff} = \frac{R4\pi^2}{gT_{eff}^2}, \qquad (1)$$

where: R is the vertical reaction (R^a, R^b).
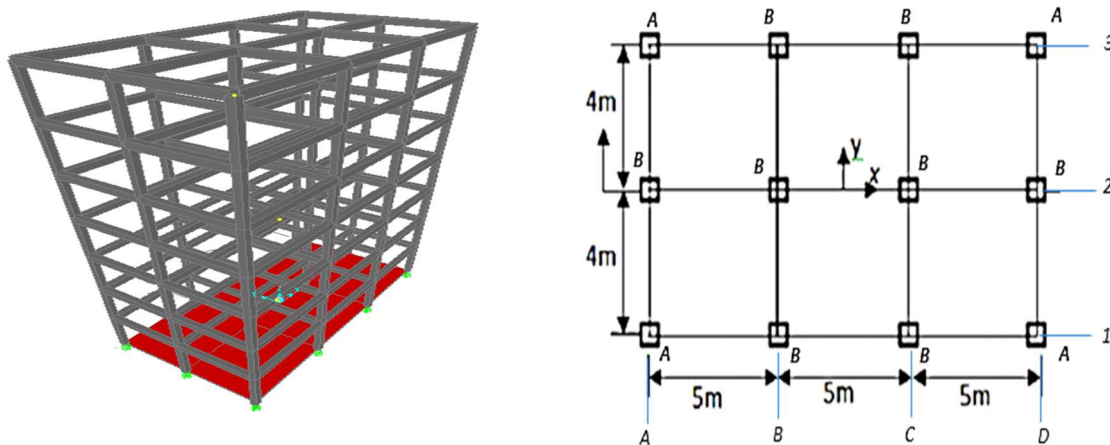
Fig. 1: a) 3D frame building, b) plan view of the structural model
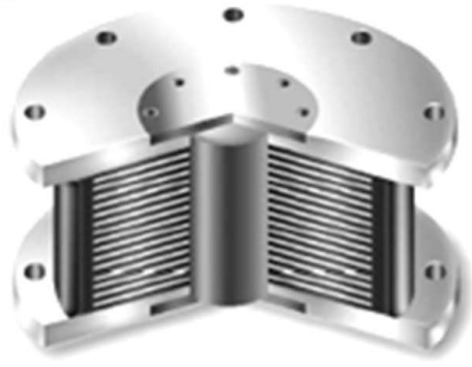
Fig. 2. Lead rubber bearing (LRB) (Takenaka Corp., Japan)

For: LRB^A $K_{eff} = \dfrac{989 \times 4 \times \pi^2}{9.81 \times 2^2}$ = 994 kN/m;

LRB^B $K_{eff} = \dfrac{1461 \times 4 \times \pi^2}{9.81 \times 2^2}$ = 1.468 kN/m.

The total effective stiffness of the isolation system can be calculated as follows:

$$\Sigma K_{eff} = 4 \times K_{eff}^A + 8 \times K_{eff}^B =$$
$$= 4 \times 994 + 8 \times 1468 = 15.720 \text{ kN/m.}$$

The design level damping ratio of the isolation system can be calculated as follows:

$$\xi = \frac{\Sigma_{eff}^A K_{eff}^A + \Sigma_{eff}^B K_{eff}^B}{4 K_{eff}^A + 8 K_{eff}^B} = 0.137, \qquad (2)$$

where ξ_{eff}^A and ξ_{eff}^B are damping ratios of individual bearings of 0.10 and 0.15, respectively.

The design displacement d_{dc} of the isolation system along the main horizontal direction is calculated as per EC8 (10.9.3) using the following expression:

$$d_{dc} = \frac{W S_e \left(T_{eff,eff} \right)}{g \Sigma K_{eff}} = 0.228 \text{ m,} \qquad (3)$$

where:

$$S_e \left(T_{eff}, \varepsilon_{eff} \right) = S_e \left(2 \text{ sec, } 13.7 \% \right) = 0.25 \text{ g;}$$

W is the total weight of the building, i.e., 14.066 kN.

The total eccentricity does not exceed 7.5 % of the length of the superstructure transverse to the horizontal direction, as specified in EC8 (Chapter 10).

$$e = e_{tot,y} = 0.05 L_i = 0.4 \text{ m} < 0.075\, L = 0.6 \text{ m}$$
(the condition is met).

L_i is the dimension of the building perpendicular to the direction of the seismic action (EC8, 4.3.2).

The total design displacement d_{db}, including torsional effects, can be calculated for each direction by multiplying the design displacement d_{dc} by given factor δi.

For the action in the x direction:

$$\delta_{xi} = 1 + \frac{e_{tot,y}}{r_y^2} y_i = 1 + \frac{0.4}{36.60} 8 = 1.07 \text{ m,} \qquad (4)$$

where:

$$r_y^2 = \Sigma(x_i^2 K_{yi} + y_i^2 K_{xi}) / \Sigma K_{xi} = 39.18 \text{ m}^2, \quad (5)$$

where y is the horizontal direction transverse to the x direction under consideration; (x_i, y_i) are the coordinates of the isolator unit i relative to the effective stiffness center (Fig. 5); $e = e_{tot, y} = 0.05 \times 8 = 0.4$ m is the total eccentricity in the y direction; r_y is the torsional radius of the isolation system in the y direction.

Total design displacement of the isolator unit:

$$d_{db} = \delta_{xi} x d_{dc} = 1.07 \times 0.228 = 0.24 \text{ m.}$$

Bilinear hysteretic behavior of the isolator

The isolation system may be modeled with bilinear hysteretic behavior, taking into account the conditions required by EC8 (EC8 S10.9.2). The bilinear model of the isolator is essentially described by three parameters: elastic stiffness (K_1), post-yield stiffness (K_2), and characteristic strength (Q). These three parameters are calculated using the convergence procedure as described below (Datta, 2010):

1. Energy dissipation per cycle, or W_D, can be estimated for very small post-yield stiffness as follows:

Fig. 3. Idealized force-deflection curve

Fig. 4. EC8 Type 1 spectrum

c.m: *center of mass*
c.s: *center of stiffness*
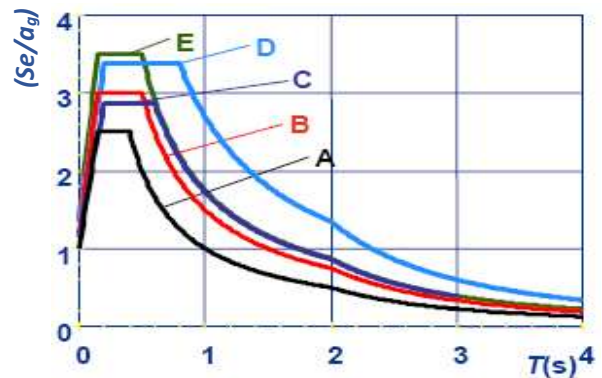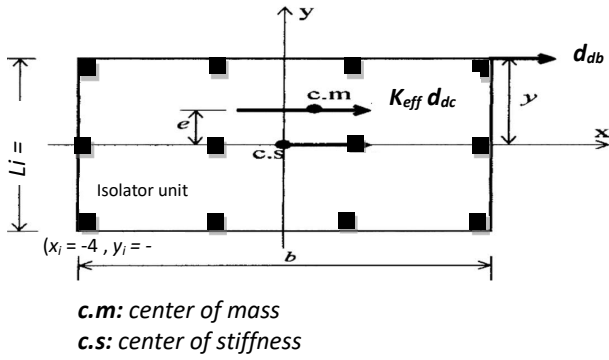
Fig. 5. Dimensions of the plan to calculate the total eccentricity

$$W_D = 2\pi K_{eff} d_{db}{}^2 \text{ and } W_D = 4Q\left(d_{db} - D_y\right). \quad (6)$$

W_D is also measured by the area bounded by the force-deflection curve loop (Fig. 3).

2. Neglecting the yield displacement D_y, the first approximation for the *short-term yield force Q* is as follows:

$$Q = \frac{\pi}{2} K_{eff} d_{db} \varepsilon_{eff}. \quad (7)$$

3. K_1 and K_2 are the pre- and post-yield stiffness ($K_1 = 10 K_2$)

$$K_2 = K_{eff} - \frac{Q}{d_{db}}. \quad (8)$$

4. D_y can be estimated as follows:

$$D_y = \frac{Q}{9K_2}. \quad (9)$$

5. Adjusting the first estimate of Q for D_y using the convergence procedure, we obtain the following:

$$Q = \frac{W_D}{4\left(d_{db} - D_y\right)}. \quad (10)$$

The properties of the isolators (LRB^A and LRB^B), designed according to EC8, after the convergence procedure are given in Table 1 and Fig. 6.

In addition, EC8 requires that the effective stiffness of the isolation system is not less than 50 % of the effective stiffness at a displacement of $0.2d_{dc}$ (EC8 S10.9.2).

$$F\left(0.2d_{db}\right) = \frac{0.2d_{db}Fy + Q\left(dy - 0.2d_{db}\right)}{d_y}; \quad (12)$$

$$\sum K_{eff}\left(0.2d_{db}\right) = 29928 \text{ kN/m};$$

$$\sum K_{eff} = 15720.00 \text{ kN/m} > 50 \text{ %};$$

$$\sum K_{eff}\left(0.2d_{db}\right) = 14.964 \text{ kN/m}$$
(the condition required by EC8 is met).

Seismic inputs and numerical analyses

The numerical analysis investigates the performance of nonlinear time history for both fixed and base-isolated building structures under 3D seismic excitations of the 1940 6.9 M_W El-Centro earthquake (PGA = 0.281 g) and the 1995 6.9 M_W Kobe earthquake (PGA = 0.834 g), classified

as far-field and near-field earthquakes, respectively (Gudainiyan and Gupta, 2023; Tamahloult and Tiliouine, 2023). The major components of each earthquake, as shown in Fig. 7, are applied in the longitudinal X direction of the building. The Nonlinear finite element software SAP2000*v*.14 (SAP, 2000) is used to obtain the dynamic responses at discrete time intervals. The solutions to the motion equations were obtained using the Fast Nonlinear Analysis method (Wilson, 2002). The isolators were modeled using LINK elements.

Seismic performance evaluation

The seismic criteria for evaluating the performance of the base-isolated building include the following parameters:

1) Peak base displacement (P_1):

$$\left(P_1\right) = \max_t \left(|d_b|\right),$$

where d_b is relative displacement with respect to the ground.

2) Story drift (P_2): the ratio between the inter-story displacement (top floor displacement d_7 and base floor displacement d_b) and the height of the building H, defined as follows:

$$\left(P_2\right) = \max_t \left(|(d_7 - d_b)|/H\right),$$

where d_7 is relative displacement of the top floor (7th floor).

3) Maximum base shear (P_3):

$$\left(P_3\right) = \max_t \left(|V_b|\right).$$
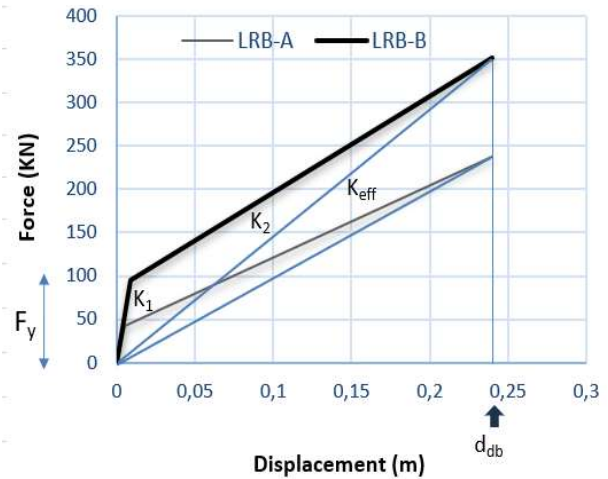
Fig. 6. Bilinear curves for the isolators LRB_A and LRB_B

Table 1. **Isolator characteristics**

Isolator characteristics	LRB$_A$	LRB$_B$
Characteristic strength, Q (kN)	38.27	86.08
Post-yield stiffness, K_2 (kN/m)	834.55	1109
Pre-yield stiffness, ($K_1 = 10 K_2$)	8345.5	11090
Yield displacement, D_y (m)	0.0051	0.0086
Yield force, $F_y = K_1 D_y$ (kN)	42.52	95.64
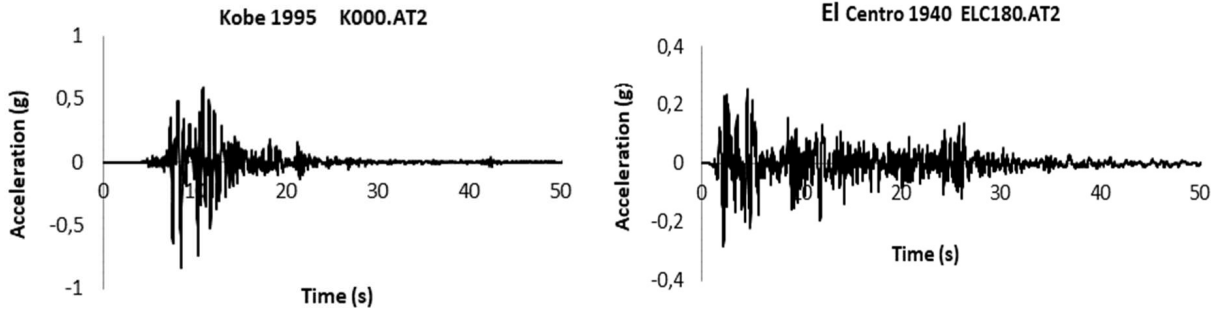
Fig. 7. Acceleration time history of longitudinal components recorded during the following earthquakes: a) Kobe, b) El-Centro

where V_b is maximum shear at the base of the building.

4) Top floor acceleration (P_4):

$$\left(P_4 \right) = \max_t \left(|a_7| \right),$$

where a_7 is total acceleration of the top floor.

5) Internal forces (bending moment values) (P_5).

Results and discussion

Table 2 summarizes the numerical results obtained from time history analyses of seismic performance for both fixed and base-isolated structures, with comments presented in the following subsections. For the sake of brevity, we only present results in the X direction (similar conclusions are found for the results in the Y direction). The findings illustrate that, in contrast to the ductility-based approach aimed at reducing earthquake damage, seismic base isolation effectively reduces maximum values of seismic inter-story drift, floor acceleration, base shear, and internal forces simultaneously, thus enhancing the structural performance of the building.

Base displacement response

The peak displacement at the base is a very important parameter in the case of base-isolated buildings, which must not exceed the predicted maximum total design displacement calculated according to EC8. The values of peak displacement in the principal direction *X* were found to be P_1 = 2.6 cm and P_1 = 15 cm for the El Centro earthquake and the Kobe earthquake, respectively. It should be noted that the peak base displacement in the case of the Kobe earthquake increased drastically, reaching up to 62 % of the total displacement. The hysteresis curves for the force displacement of LRB[B] bearings are presented in Fig. 8a and Fig. 8b for the El-Centro

and Kobe earthquakes, respectively. It is evident that the bilinear behavior assumption according to EC8 is compatible with the force-deformation curves of the seismic isolator obtained from the time history analyses.

Inter-story drift displacement response

The drift ratio in the base-isolated structure shows a minor reduction in the case of the El Centro earthquake but a significant reduction of about 53 % during the Kobe earthquake, as shown in Table 2. However, in the case of the fixed-base building, the drift ratio calculated for the Kobe earthquake is equal to 0.8 %, which is very close to the EC8 requirement limit (0.005/v = 1 %). This result illustrates the effectiveness of the LRB isolation in reducing the drift displacement of the structure and suggests that the superstructure behaves similarly to a rigid body when placed above the isolation system.

Base shear response

The results of the base shear time history demonstrate a significant reduction due to the incorporation of an isolation system. For example, in the case of the El Centro earthquake, the peak base shear values for the base-isolated building and its fixed base are 1.089 kN and 1.290 kN, respectively. In the case of the Kobe earthquake, the base shear values are 2.504 kN and 3.433 kN, respectively, as shown in Fig. 9.

Absolute acceleration response

The comparison of maximum top floor accelerations between fixed-base and isolated-base structures is presented in Table 2. In the X direction, the maximum top floor acceleration decreased from P_4 = 7.77 m/s² to P_4 = 5.25 m/s² for the El Centro earthquake

Table 2. **Seismic performance of fixed and base-isolated buildings**

Seismic performance evaluation	El-Centro (PGA = 0.281 g)		KOBE (PGA = 0.834 g)	
	Fixed base	Base-isolated	Fixed base	Base-isolated
Base displacement (P_1) (cm)	–	2.30	–	14.9
Roof drift (P_2)	0.0031	0.0032	0.0085	0.0066
Base shear (P_3) (kN)	1290	1089	3433	2504
Top floor acceleration (P_4) (m²/s)	7.77	5.25	20.23	10.03
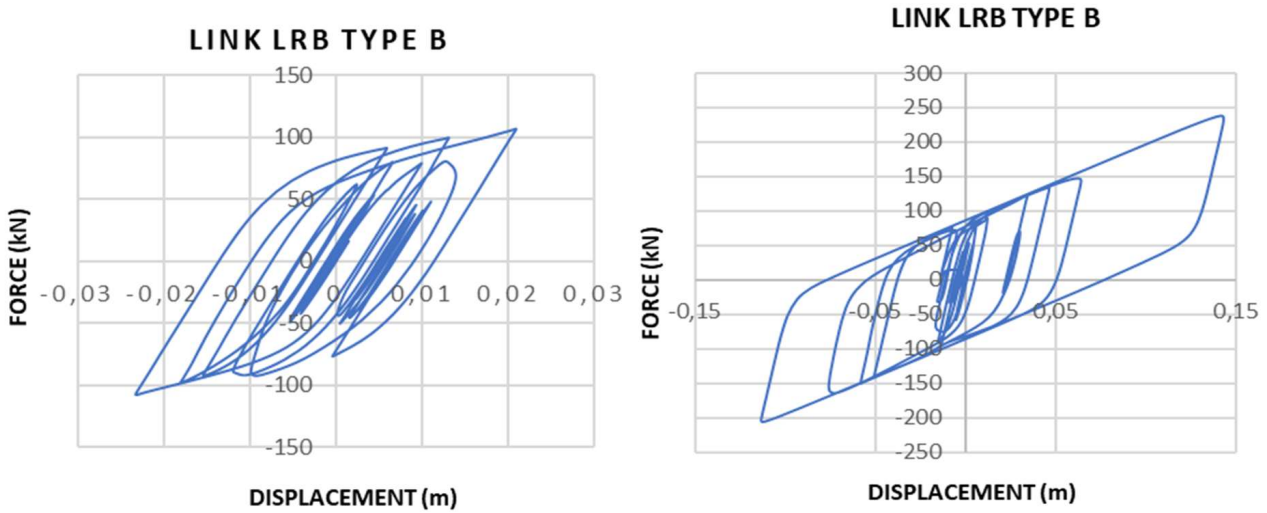
Fig. 8. Force-deformation curves of the seismic isolator for 3D input acceleration ground motion components recorded during the El Centro (a) and Kobe (b) earthquakes

(a reduction of 32 %) and from P_4 = 20.23 to P_4 = 10.03 m/s² for the Kobe earthquake (a reduction of 50 %). This decrease in absolute acceleration for the base-isolated structure demonstrates the effectiveness of the isolation system.

Internal forces (bending moment values)

Table 3 presents the calculated values of the maximum bending moments in the fixed-base and base-isolated building structures for both the El-Centro and Kobe earthquakes. It has been observed that for the base-isolated building, there is a significant reduction in bending moment values compared to those of the fixed-base building, as shown in Table 3, for both load cases, the El-Centro and Kobe earthquakes. For example, at the base level, the maximum bending moments decrease from 302 to 222 kN·m and from 829 to 631 kN·m for the El Centro and Kobe earthquakes, respectively. Furthermore, at the top level, a significant reduction of approximately 50 % can be observed. For example, the maximum bending moments decrease from 42 kN·m to 28 kN·m for the El Centro earthquake and from 113 kN·m to 53 kN·m for the Kobe earthquake.

These results once again demonstrate the success of LRB bearings in controlling internal forces under both gravity and seismic loads. As a result, it may be interesting to consider the possibility of resizing the cross-sectional dimensions of structural elements, especially columns and beams (all beams 35×30 cm², all columns 40×40 cm²), within the base-isolated building. This adjustment has the potential to enhance structural efficiency and yield cost savings.

Conclusion

The design of base isolation systems is well defined in EC8 for building structures. The design displacement of an isolator unit is calculated using a formula defined in EC8, depending on the spectral acceleration (type 1 spectrum). This formula includes several parameters such as the reference peak ground acceleration of each seismic zone, the soil factor S, the behavior factor, the importance factor of buildings, effective fundamental period, and effective damping. The dynamic response behavior of a multi-story building structure isolated using an LRB system was evaluated. Seismic response parameters for structures with fixed and isolated
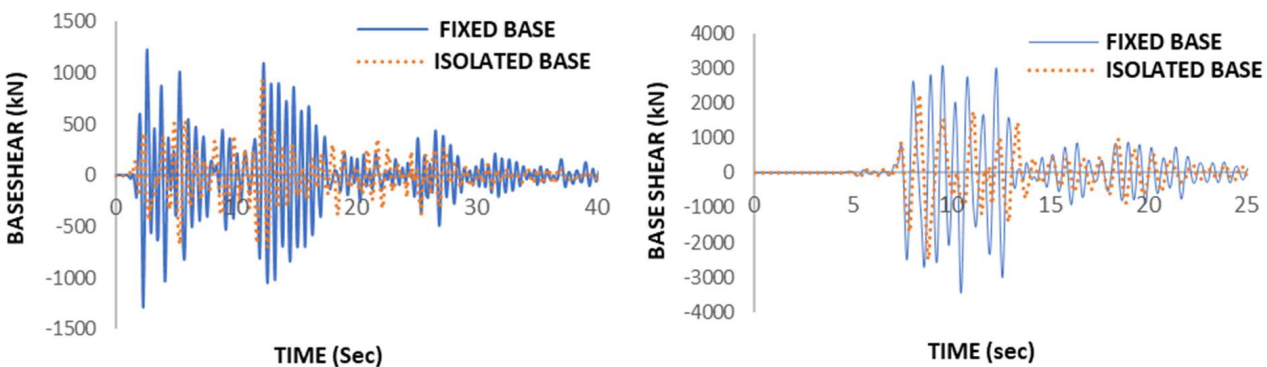
Fig. 9. Comparison of base shear between fixed-base and base-isolated buildings for the El Centro (a) and Kobe (b) earthquakes

Table 3. **Maximum bending moment values**

Maximum bending moment values		El-Centro (PGA = 0.281 g)		KOBE (PGA = 0.834 g)	
		Fixed base	Base-isolated	Fixed base	Base-isolated
1st story	Column	302	222	829	631
	Beam	144	189	397	433
2nd story	Column	224	205	618	444
	Beam	178	155	488	321
3rd story	Column	190	170	523	347
	Beam	174	120	476	268
4th story	Column	189	127	511	295
	Beam	149	89	408	212
5th story	Column	165	96	449	254
	Beam	115	67	308	157
6th story	Column	127	81	340	189
	Beam	74	47	198	96
7th story	Column	82	46	219	118
	Beam	42	28	113	53

bases were evaluated in accordance with the provisions outlined in EC8. The output results clearly demonstrate the effectiveness of the isolator system in significantly and simultaneously reducing seismic responses, including floor accelerations, inter-story drifts, and base shear. In addition, it was observed that the isolation system with LRB bearings reduces internal forces caused by both gravity and seismic loads. As a result, it may be useful to consider the possibility of resizing the cross-sectional dimensions of structural elements, especially columns and beams, within the base-isolated building. This adjustment has the potential to enhance structural efficiency and yield cost savings.

References

AASHTO (2010). *Guide specifications for seismic isolation design*. 3rd edition. Washington, DC: AASHTO, 47 p.

Amanollah, F., Ostrovskaya, N., and Rutman, Y. (2023). Structural and parametric analysis of lead rubber bearings and effect of their characteristics on the response spectrum analysis. Architecture and Engineering, Vol. 8, No. 1, pp. 37–43. DOI: 10.23968/2500-0055-2023-8-1-37-43.

Asher, J. W., Hoskere, S. N., Ewing, R. D., Mayes, R. L., Button, M. R., and Van Volkinburg, D. R. (1997). Performance of seismically isolated structures in the 1994 Northridge and 1995 Kobe earthquakes. Building to Last, Leon Kempner, Jr. and Colin B. Brown, Editors, Proc. of Structures Congress XV, Published by ASCE, 1128-1132.

Attanasi, G., Auricchio, F., and Fenves, G. L. (2009). Feasibility assessment of an innovative isolation bearing system with shape memory alloys. *Journal of Earthquake Engineering*, Vol. 13, Issue S1, pp. 18–39. DOI: 10.1080/13632460902813216.

Cavdar, E. and Ozdemir G. (2022). Amplification in maximum isolator displacement of an LRB isolated building due to mass eccentricity. *Bulletin of Earthquake Engineering*, Vol. 20, pp. 607–631. DOI: 10.1007/s10518-021-01247-1.

Cheng, F. Y., Jiang, H., and Lou, K. (2008). *Smart structures. Innovative systems for seismic response control*. Boca Raton: CRC Press, 672 p.

SAP2000 Integrated software for structural analysis and design. (2000). Computers and Structures Inc. Computer software, Berkeley, California, USA.

Datta, T. K. (2010). *Seismic analysis of structures*. Singapore: John Wiley & Sons (Asia) Pte Ltd, 464 p.

Elghazouli, A. Y. (ed.). (2009). *Seismic design of buildings to Eurocode 8*. 2nd edition. Boca Raton: CRC Press, 363 p.

European Committee for Standardization (2004). *Eurocode 8: Design of structures for earthquake resistance. Part 1: General rules, seismic actions and rules for buildings*. Brussels: European Committee for Standardization, 230 p.

Gudainiyan, J. and Gupta, P. K. (2023). Effect of frequency content parameter of ground motion on the response of C-shaped base-isolated building. *Asian Journal of Civil Engineering*, Vol. 24, pp. 2973–2983. DOI: 10.1007/s42107-023-00688-0.

Hu, G.-J., Ye, K., and Tang, Z.-Y. (2023). Design and analysis of LRB base-isolated building structure for multilevel performance targets. *Structures*, Vol. 57, 105236. DOI: 10.1016/j.istruc.2023.105236.

Jain, S. K. (2004). Seismic isolation devices: a review. *Bridge and Structural Engineer (IABSE)*, Vol. 34, Issue 2, pp. 19–47.

Kelly, J. M. (1997). *Earthquake-resistant design with rubber*. 2nd edition. London: Springer, 243 p. DOI: 10.1007/978-1-4471-0971-6.

Koo, G.-H., Lee, J.-H., Lee, H.-Y., and Yoo, B. (1999). Stability of laminated rubber bearing and its application to seismic isolation. *KSME International Journal*, Vol. 13, Issue 8, pp. 595–604. DOI: 10.1007/BF03184553.

Mayes, R. L. and Naeim, F. (2001). Design of structures with seismic isolation. In: Naeim, F. (ed.). *The Seismic Design Handbook*. Boston: Springer, pp. 723–755. DOI: 10.1007/978-1-4615-1693-4_14.

Ministry of Housing and Urban-Rural Development of the People's Republic of China (2010). *GB50011-2010. Code for seismic design of buildings*. Beijing: Ministry of Housing and Urban-Rural Development of the People's Republic of China, 228 p.

Mori, A., Moss, P. J., Carr, A. J., and Cooke, N. (1998). Behaviour of lead-rubber bearings. Structural *Engineering and Mechanics*, Vol. 6, No. 1, pp. 1–15. DOI: 10.12989/sem.1998.6.1.001.

Naeim, F. and Kelly, J. M. (1999). *Design of seismic isolated structures: from theory to practice*. New York: John Wiley & Sons, Inc., 304 p.

Tamahloult, M. and Tiliouine, B. (2023). 3D nonlinear seismic analysis and design of base-isolated buildings under near field ground motions. *Građevinar*, Vol. 75, No. 5, pp. 483–493. DOI: 10.14256/JCE.3548.2022.

Wilson, E. L. (2002). *Three-dimensional static and dynamic analysis of structures*. 3rd edition. Berkeley: Computers and Structures Inc., 423 p.

ВЛИЯНИЕ СИСТЕМ СЕЙСМОИЗОЛЯЦИИ НА ОСНОВЕ СВИНЦОВО-РЕЗИНОВЫХ ОПОР НА СТРОИТЕЛЬНЫЕ КОНСТРУКЦИИ, СПРОЕКТИРОВАННЫЕ В СООТВЕТСТВИИ С ЕВРОКОДОМ 8

Мохаммед Тамалулт[1], Мулуд Уанани [2], Буалем Тилиуин[1]*

[1]Лаборатория сейсмостойкого строительства и динамики сооружений, факультет гражданского строительства
Национальная политехническая школа, Алжир

[2]Факультет гражданского строительства
Университет Джельфы, Алжир

*E-mail: boualem.tiliouine@g.enp.edu.dz

Аннотация
Введение: Сейсмоизоляция представляет собой систему защиты сооружений, минимизирующую воздействие сейсмических сил на сооружение во время землетрясения. Этого можно достичь с помощью различных устройств, таких как эластомерные опоры, скользящие опоры и гибридные системы. **Цель исследования**: оценить влияние свинцово-резиновых опор, используемых в строительных конструкциях в качестве системы сейсмоизоляции. **Методы:** для достижения указанной цели, с помощью алгоритма Fast Nonlinear Analysis (FNA) был проведен нелинейный динамический анализ семиэтажного здания с изолирующим устройством в основании и без него. Здание спроектировано в соответствии с критериями Еврокода 8 (EC8), а затем подвергнуто анализу с использованием данных о двух произошедших землетрясениях. **Результаты**: сделан вывод о том, что допущение о билинейном поведении, сделанное на этапе проектирования в соответствии с EC8, является обоснованным. Кроме того, применение системы сейсмоизоляции фундамента здания с использованием свинцово-резиновых опор может значительно улучшить эксплуатационные характеристики здания за счет уменьшения ускорений перекрытий, межэтажных перекосов и горизонтальной сейсмической реакции. Кроме того, показано, что сейсмоизоляция здания с помощью свинцово-резиновых опор эффективно уменьшает внутренние силы, возникающие как от гравитационных, так и от сейсмических нагрузок.

Ключевые слова: сейсмоизоляция; система свинцово-резиновых опор; трехмерный анализ нелинейной реакции на землетрясение; Еврокод 8; билинейный гистерезис.